Available online at www.sciencedirect.com
SCIENCE DIRECT®
Journal of the European Ceramic Society 25 (2005) 1705–1715
www.elsevier.com/locate/jeurceramsoc

Rare earth silicate environmental barrier coatings for SiC/SiC composites and Si_3N_4 ceramics

Kang N. Lee*, Dennis S. Fox, Narottam P. Bansal

NASA Glenn Research Center, Cleveland, OH 44135, USA

Available online 21 January 2005

Abstract

Rare earth silicates have been investigated to evaluate their potential as an advanced environmental barrier coating (EBC) having higher temperature capability than current EBCs. Volatility data in high steam environments indicate that rare earth monosilicates (RE_2SiO_5; RE: rare earth element) have lower volatility than the current barium strontium aluminum silicate (BSAS) EBC top coat in combustion environments. Rare earth silicates also exhibit superior chemical compatibility compared to BSAS. The superior chemical compatibility and low volatility are key attributes to achieve higher temperature capability. The chemical compatibility is especially critical for EBCs on Si_3N_4 because of the high chemical reactivity of some of the oxide additives in Si_3N_4. In simulated combustion environments, EBCs with a rare earth monosilicate top coat exhibit superior temperature capability and durability compared to the current state-of-the art EBCs with a BSAS top coat.

Keywords: SiC; Si_3N_4; Environmental barrier coating

1. Introduction

A major breakthrough in gas turbine engine performance (efficiency and emission) requires a new generation of hot section structural materials having a temperature capability considerably higher than current metallic hot section structural materials. It is generally agreed that the temperature capability of Ni-base metals has reached their limit. Ceramic thermal barrier coatings are used to insulate metallic components, thereby allowing higher gas temperatures, but the metallic component remains a weak link because the designer must allow for the possibility of coating loss from spallation or erosion. Si-based ceramics, such as silicon carbide (SiC) fiber-reinforced SiC ceramic matrix composites (SiC/SiC CMCs) and monolithic silicon nitride (Si_3N_4), exhibit superior high-temperature strength and durability, indicating their potential to revolutionize gas turbine engine technology. A key stumbling block to realizing Si-based ceramic turbine hot section components is their lack of environmental durability in high velocity combustion environments. The silica scale, normally responsible for their excellent high temperature oxidation resistance in dry air, reacts with water vapor, a byproduct of combustion reactions, and forms gaseous silicon hydroxide species.[1,2] This results in unacceptably high recession rate of Si-based ceramics. This can be prevented by an environmental barrier coating (EBC) which is an external barrier coating whose prime purpose is to prevent Si-based ceramics from reacting with water vapor.[3]

Mullite attracted the most interest as a protective coating for SiC or Si_3N_4 ceramics in the early days of coating development due to its low coefficient of thermal expansion (CTE), chemical compatibility with Si-based ceramics, and good adherence.[3–7] One key issue with plasma-sprayed mullite coatings is the phase stability.[7] Mullite processed with conventional plasma spraying contains a significant amount of metastable amorphous phase due to the rapid cooling of molten mullite during its solidification on a cold substrate. A subsequent exposure of the mullite coating to a temperature above ~1000 °C causes crystallization of the amorphous phase. Shrinkage accompanies the crystallization, leading to cracking and delamination of the mullite coating. A second generation, fully crystalline plasma-sprayed mullite coating was developed by spraying the coating while the substrate was maintained above the amorphous mullite crystallization

* Corresponding author. Present address: Cleveland State University, Cleveland, OH, USA. Tel.: +1 216 433 5634; fax: +1 216 433 5544.
E-mail address: Kang.N.Lee@grc.nasa.gov (K.N. Lee).

0955-2219/$ – see front matter © 2004 Elsevier Ltd. All rights reserved.
doi:10.1016/j.jeurceramsoc.2004.12.013

temperature.[7] Consequently, the second generation mullite coating exhibits dramatically enhanced adherence and crack resistance. Another major issue with the mullite coating is the relatively high silica activity (∼0.4) and the resulting recession in high velocity combustion environments due to the selective volatilization of silica by water vapor.[8] The selective volatilization of silica from the mullite leaves a porous alumina surface layer which readily spalls.

One way to overcome the recession of mullite is by adding a water-vapor resistant top coat. Yttria-stabilized zirconia (YSZ) is a logical top coat candidate because of its track record as a successful thermal barrier coating (TBC) for metallic components in gas turbine engines, signifying its stability in water vapor. Consequently, the first generation water vapor-resistant EBC was developed by adding an YSZ (ZrO_2-8 wt.% Y_2O_3) top coat.[8] One critical weakness of YSZ is its large CTE, twice that of SiC or mullite. This first generation EBC provided protection from water vapor for a few hundred hours at ∼1300 °C. In longer exposures under thermal cycling, however, the CTE mismatch causes severe cracking and delamination, leading to premature EBC failure.

Second generation EBCs, with substantially improved durability, were developed in the NASA High Speed Research-Enabling Propulsion Materials (HSR-EPM) Program in joint research between NASA, General Electric and Pratt & Whitney.[9,10] The YSZ top coat was replaced with BSAS ($1\text{-}x\text{BaO}\text{-}x\text{SrO}\text{-}Al_2O_3\text{-}2SiO_2$, $0 \le x \le 1$) which exhibited superb crack resistance due to reduced tensile stress resulting from the low CTE and low modulus of BSAS.[11] Adding BSAS second phase in the mullite coating also significantly reduced the tensile stress, resulting in far superior crack resistance compared to the unmodified mullite coating.[11] Another innovation in second generation EBCs was the development of a Si bond coat which further enhanced the EBC performance by providing significantly improved adherence. Consequently, the second generation EBCs consist of three layers: a silicon bond coat, a mullite or a mullite + BSAS intermediate coat, and a BSAS top coat. EBC stress evolution and its effects on EBC durability is discussed in detail in ref.[11]

The second generation EBCs have been scaled up and applied on SiC/SiC CMC combustor liners used in three Solar Turbine (San Diego, CA) Centaur 50s gas turbine engines under the DOE Ceramic Stationary Gas Turbines (CSGT) Program.[12,13] The combined operation of the three engines has resulted in the accumulation of over 24,000 h without failure by the end of 1999 (∼1250 °C maximum combustor liner temperature). One engine used by Texaco in Bakersfield, CA successfully completed a 14,000-h field test. The higher operating temperature resulted in emissions consistently below 15 ppmv nitrogen oxides (NO*x*) and below 10 ppmv carbon monoxide (CO) throughout, roughly reducing the NO*x* and CO loads on the environment by factors of about 2 and 5, respectively.

Second generation EBCs have some durability issues that limit their use temperature and life.[10] One key issue is the volatilization of the BSAS top coat in high velocity combustion environments. A projection based on a silica volatility model[2] in conjunction with BSAS volatility data from high steam low velocity environments indicates a BSAS recession of ∼70 μm after 1000 h at 1400 °C, 6 atm total pressure, and 24 m/s gas velocity.[10] Actual gas turbines operate at significantly higher pressures and gas velocities, increasing the projected recession to much higher levels. In fact the EBC on Solar Turbine engines suffered significant BSAS recession in some areas after the 14,000 h test.[13] Another key durability issue is the chemical reaction between BSAS and silica formed on the Si bond coat by oxidation. The BSAS-silica reaction generates a low-melting (∼1300 °C) glass that causes EBC degradation and premature failure at temperatures above ∼1300 °C.[10]

Research has been undertaken at the NASA Glenn Research Center under the support of the Ultra Efficient Engine Technology (UEET) Program to develop EBCs that can withstand a 1482 °C (2700 °F) surface temperature and sustain 1316 °C (2400 °F) EBC/substrate temperature over thousands of hours. The research has focused on identifying a new top coat, to replace the current BSAS top coat, that has 2700 °F temperature capability and chemical/mechanical compatibility with the mullite or mullite + BSAS intermediate coat at 1400 °C (2552 °F) or higher. Some rare earth silicates have been identified as promising candidates due to their low CTE and phase stability. Table 1 lists the CTE of low CTE rare earth silicates determined in this study along with the CTE of current EBCs. It has been reported that rare earth disilicate ($RE_2Si_2O_7$, RE: rare earth element) of Y, Tm, Er, and Ho has several polymorphs,[14,15] while $Lu_2Si_2O_7$ has no polymorphs.[16] Among rare earth monosilicates (RE_2SiO_5, RE: rare earth element), Sc, Lu, Yb, Tm, Er, and Dy do not have polymorphs, while the other rare earth monosilicates have two polymorphs with a substantial disparity in density between the two polymorphs.[17] Materials having polymorphs with differing density are not desirable coating candidates since volume change accompanies the phase transformation. It appears that rare earth monosilicates with relatively low CTE happen to have phase stability as well, making them promising EBC candidates.

Table 1
CTE of SiC and various EBC materials

Material	Average CTE ($\times 10^{-6}$ °C)
Y_2SiO_5	5–6
Er_2SiO_5	5–7
Yb_2SiO_5	3.5–4.5
Lu_2SiO_5	TBD[a]
$Sc_2Si_2O_7 + Sc_2O_3$	5–6
$Yb_2Si_2O_7$	TBD[a]
Mullite	5–6
BSAS (monoclinic celsian)	4–5
BSAS (hexagonal celsian)	7–8
Si	3.5–4.5
SiC, SiC/SiC	4.5–5.5
Si_3N_4	3–4

[a] To be determined.

Volatility of Y, Yb, and Lu disilicates has been investigated in high velocity and high steam environments at 1450–1500 °C.[16,18,19] These disilicates gradually decomposed to monosilicates due to selective volatilization of silica. To the best of our knowledge no volatility data for rare earth monosilicates in combustion environments have been reported in the literature. This paper will discuss the volatility of selected low CTE rare earth disilicates and monosilicates in high steam environments and their performance as an EBC on SiC/SiC composite and Si_3N_4 ceramics in simulated combustion environments.

2. Experimental

EBCs were applied by atmospheric pressure plasma spraying onto sintered α-SiC coupons (Hexoloy™, Carborundum, Niagara Falls, NY), melt infiltrated (MI) SiC/SiC CMC[20] (GE Power Generation Composites, Newark, Delaware) and sintered Si_3N_4 (AS800™, Honeywell Engines, Phoenix, AZ). The monolithic SiC was etched in molten Na_2CO_3 to create a rough surface (R_a[a] = 5–6 μm) necessary for good mechanical bond with the coating.[7] The MI SiC/SiC CMC and AS800™ Si_3N_4 were used as processed. Silicon powder was purchased from Atlantic Equipment Engineers (Bergenfield, NJ), mullite powder from Cerac Inc. (Milwaukee, WI), BSAS powder from H.C. Starck Inc. (Newton, MA), and rare earth silicate powder from Praxair Specialty Ceramics (Woodinville, WA). Two types of silicon bond coat were used: the silicon surface layer already present on as-processed MI SiC/SiC with the thickness ranging from a few μm to ∼100 μm; or a plasma-sprayed silicon, typically 50–75 μm (2–3 mils) thick. The subsequent coating layers were ∼125 μm (5 mil) thick each. Details of the coating process parameters are described elsewhere.[7]

The volatilization of EBC top coat candidates were investigated by thermogravimetric analysis (TGA) of hot-pressed monolithic EBC coupons. Hot pressing was performed at 1500 °C/4 ksi in vacuum using powders with the particle size of 1–5 μm. TGA was conducted in 50% H_2O-50% O_2 flowing at 4.4 cm/s in 1 atm total pressure at 1500 °C. Volatilization kinetics was measured with a continuously recording Cahn 1000 microbalance (Cerritos, CA). Sample size was nominally 2.5 cm × 1.25 cm × 0.15 cm. EBC performance was evaluated by exposing EBC-coated coupons to thermal cycling in simulated lean combustion environments. All EBC-coated coupons were annealed in air at 1300 °C for 20 h prior to testing to stabilize coating phases. Most thermal cycling tests were conducted at 1300 °C (or 1316 °C) and 1380 °C in 90% H_2O-balance O_2, flowing at 2.2 cm/s at 1 atm total pressure, using automated thermal cycling furnaces. Details of the automated thermal cycling furnace are described in ref.[10] The choice of 1380 °C as the upper test temperature, instead of 1400 °C which is the goal temperature at the top coat/intermediate coat interface, was to avoid accidental melting of the Si bond coat whose melting point is 1416 °C for pure Si and lower when contaminated. A few selected samples were exposed to 1400 °C or higher to evaluate chemical compatibility at higher temperatures. Each thermal cycle consisted of 1 h at temperature, rapid cooling to room temperature, and 20 min at room temperature. Samples reached peak temperature within 2 min (∼700 °C/min), and cooled to room temperature within 5 min (∼300 °C/min) in each cycle. Sample size for thermal cycling tests was nominally 2.5 cm × 0.6 cm × 0.15 cm.

3. Results and discussion

3.1. Volatility in water vapor

3.1.1. BSAS, SAS, and BAS

Fig. 1 is a plot of weight change versus time for hot-pressed BSAS family materials exposed to 50% H_2O-balance O_2 flowing at 4.4 cm/s at 1500 °C and 1 atm total pressure. BAS ($BaO\text{-}Al_2O_3\text{-}2SiO_2$) shows the highest volatility followed by SAS ($SrO\text{-}Al_2O_3\text{-}2SiO_2$) and BSAS. The volatility and the resulting recession at higher flow rates and system pressures experienced in actual gas turbines can be projected by using a silica volatility model[2] in conjunction with the volatility data from Fig. 1. The projected recession of BSAS after 1000 h at 6 atm total pressure and 24 m/s gas velocity is 30, 70, and 270 μm at 1300, 1400, and 1500 °C, respectively.[10] Higher recession is expected for BAS or SAS. These recession rates are unacceptably high for long-term durability (over thousands of hours) in advanced gas turbines.

3.1.2. Rare earth silicates

Fig. 2a and b are plots of weight change versus time for various hot-pressed rare earth silicates exposed to 50% H_2O-balance O_2 flowing at 4.4 cm/s at 1500 °C and 1 atm total pressure. The volatility of BSAS is included in Fig. 2 for comparison. The starting raw materials (rare earth oxide and silica) were mixed in a ratio to produce rare earth monosilicates (RE_2SiO_5; RE: rare earth element) when completely reacted. Table 2 shows the phases in rare earth silicates determined by X-ray diffraction before and after exposure. Ytterbium, lutetium, erbium, and yttrium silicates contained

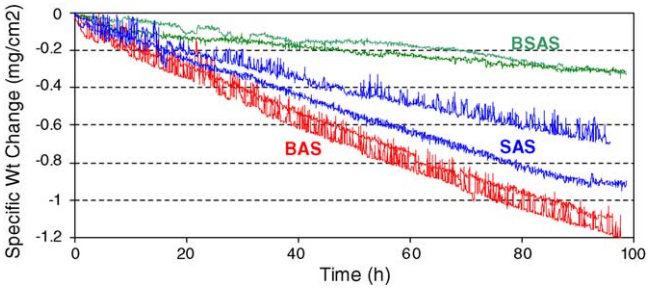

Fig. 1. Volatility of hot-pressed BSAS family materials exposed to 50% H_2O-balance O_2 flowing at 4.4 cm/s at 1500 °C and 1 atm total pressure.

[a] Average distance from the roughness profile to the mean line.

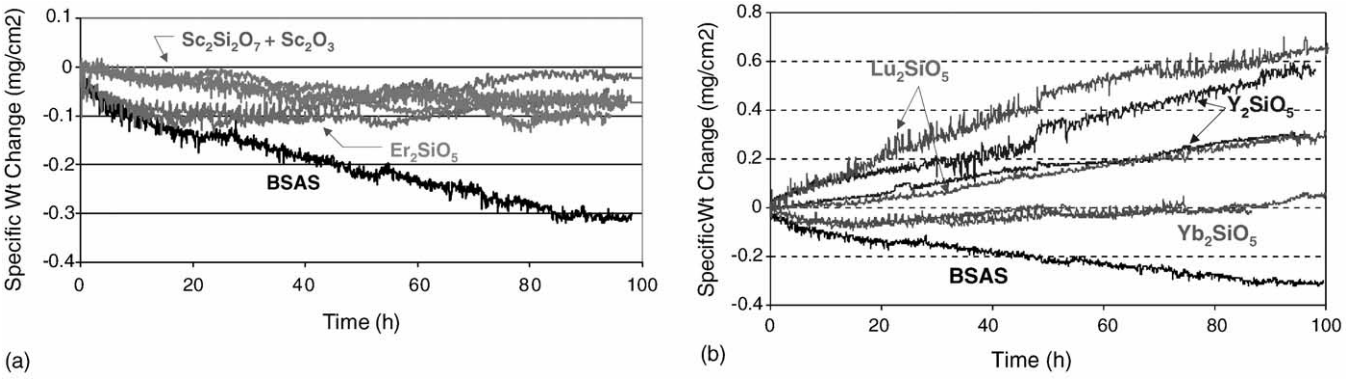

Fig. 2. Volatility of hot-pressed rare earth silicates exposed to 50% H_2O-balance O_2 flowing at 4.4 cm/s at 1500 °C and 1 atm total pressure.

mostly monosilicate phase with a trace amount of unreacted rare earth oxide and disilicate, whereas disilicate and rare earth oxide were the major phases with a trace amount of monosilicate in scandium silicate. This indicates that either Sc_2SiO_5 is unstable and readily decomposes to disilicate and oxide on cooling, or the reaction kinetics to form Sc_2SiO_5 is very sluggish. The weight of Yb_2SiO_5 and Er_2SiO_5 remained fairly flat, while Y_2SiO_5 and Lu_2SiO_5 showed a slight weight gain and $Sc_2Si_2O_7 + Sc_2O_3$ showed a slight weight loss. Post-exposure Y_2SiO_5, Yb_2SiO_5, Er_2SiO_5, and Lu_2SiO_5 showed a trace amount of alumina-containing compound. The reaction chamber is an alumina tube and alumina is known to react with water vapor to form aluminum hydroxides.[21] Therefore, alumina-containing compounds are believed to be due to the reaction between RE_2SiO_5 and aluminum hydroxides in the vapor phase. Post-exposure $Sc_2Si_2O_7 + Sc_2O_3$ did not show any reaction products, indicating that the small weight loss is due to the volatility of $Sc_2Si_2O_7$.

Fig. 3 shows the volatility of two rare earth disilicates ($Sc_2Si_2O_7$ and $Yb_2Si_2O_7$) exposed to 50% H_2O-balance O_2 flowing at 4.4 cm/s at 1500 °C and 1 atm total pressure. Both disilicates and BSAS showed a similar weight loss within the experimental scatter. $Sc_2Si_2O_7$ did not show any reaction products while $Yb_2Si_2O_7$ showed a trace amount of alumina-containing compound.

The contamination by alumina makes it difficult to make unequivocal conclusions on the volatility of rare earth silicates except for Sc silicates: $Sc_2Si_2O_7$ has volatility similar to

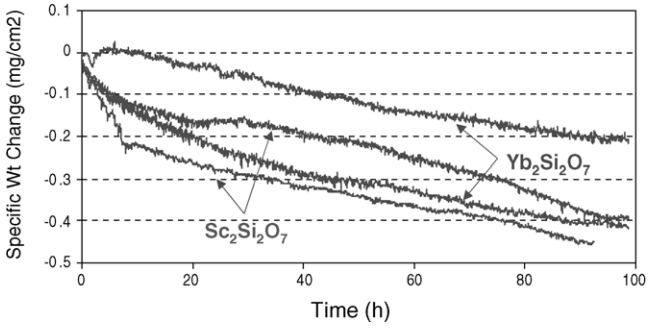

Fig. 3. Volatility of hot-pressed rare earth disilicates ($Sc_2Si_2O_7$ and $Yb_2Si_2O_7$) exposed to 50% H_2O-balance O_2 flowing at 4.4 cm/s at 1500 °C and 1 atm total pressure.

that of BSAS and therefore Sc_2SiO_5 has lower volatility than BSAS. It is likely that the other rare earth monosilicates are also less volatile than BSAS since all rare earth monosilicates are likely to have similar silica volatility. Thermodynamic calculations have shown that the silica activity of $Dy_2Si_2O_7$ and Dy_2SiO_5 at 1500 °C is ~0.3 and ~0.01, respectively, and further decreases with decreasing temperature.[22] The very low silica activity of Dy_2SiO_5 is consistent with the low silica volatility suggested for rare earth monosilicates. A volatility test that eliminates the contamination of test samples is necessary to unequivocally determine the volatility of rare earth silicates.

Table 2
Phases in hot-pressed EBC materials by X-ray diffraction before and after a 100-h exposure to 50% H_2O-50% O_2 flowing at 4.4 cm/s in 1 atm total pressure at 1500 °C

Material	As-processed	Post-exposure
Y_2SiO_5	$Y_2SiO_5 + Y_2O_3$[a] + $Y_2Si_2O_7$[a]	Y_2SiO_5, $Al_2Y_4O_9$[b]
Er_2SiO_5	$Er_2SiO_5 + Er_2O_3$[a] + $Er_2Si_2O_7$[a]	Er_2SiO_5, $Al_{10}Er_6O_{24}$[b]
Yb_2SiO_5	$Yb_2SiO_5 + Yb_2O_3$[a] + $Yb_2Si_2O_7$[a]	Yb_2SiO_5, $Al_5Yb_3O_{12}$[b]
Lu_2SiO_5	Lu_2SiO_5	Lu_2SiO_5, $Al_5Lu_3O_{12}$[b]
$Sc_2Si_2O_7 + Sc_2O_3$	$Sc_2Si_2O_7$, Sc_2O_3, Sc_2SiO_5[a], SiO_2[a]	$Sc_2Si_2O_7$, Sc_2O_3, Sc_2SiO_5[a]
$Sc_2Si_2O_7$	$Sc_2Si_2O_7$, SiO_2[a]	$Sc_2Si_2O_7$
$Yb_2Si_2O_7$	$Yb_2Si_2O_7$, Yb_2SiO_5[a]	$Yb_2Si_2O_7$, Yb_2SiO_5[a], $Al_5Yb_3O_{12}$[b]
BSAS	Monoclinic celsian	Monoclinic celsian

[a] Trace amount.
[b] Trace amount, from reaction with Al_2O_3 tube used during exposure.

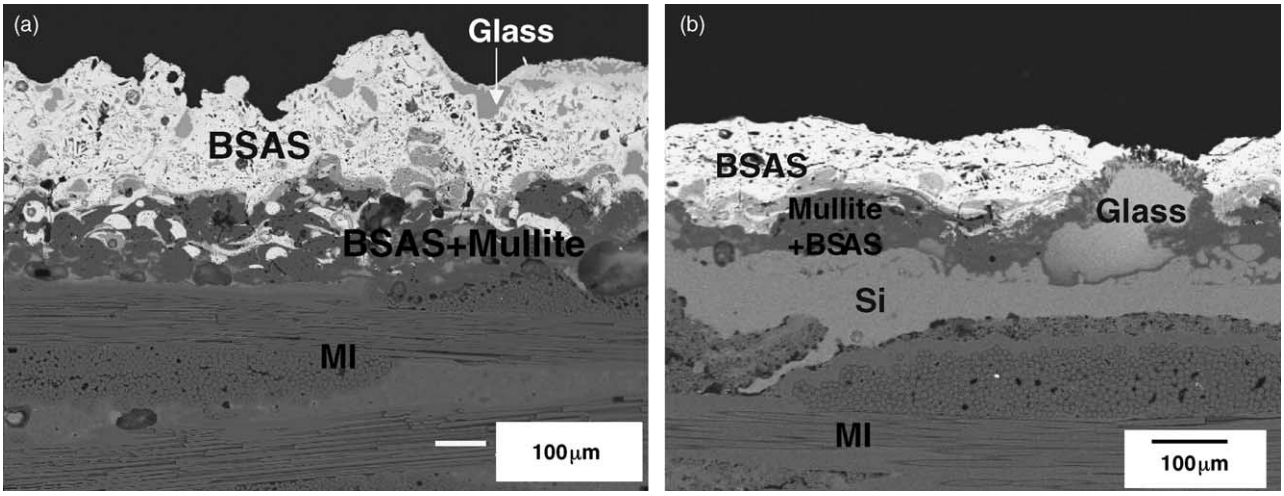

Fig. 4. Cross-sections of Si/mullite + BSAS/BSAS EBC on MI SiC/SiC composite in 90% H_2O-balance O_2 after 1000 h-1316 °C-1 h cycles (a) and 300 h-1400 °C-1 h cycles (b).

3.2. Chemical stability/environmental durability—SiC or SiC/SiC composite substrate

3.2.1. Mullite + BSAS family/BSAS EBC

Fig. 4a and b shows cross-sections of Si/mullite + BSAS/BSAS EBC on MI SiC/SiC composite in 90% H_2O-balance O_2 after 1000 h-1316 °C (1 h cycles) and 300 h-1400 °C (1 h cycles) exposures, respectively. Both maintained excellent adherence and oxidation resistance. Patches of glass phase (areas with darker contrast) are clearly noticeable in the BSAS top coat in Fig. 4a. The glass formation becomes more active at 1400 °C, converting significant portions of EBC into glass (Fig. 4b). The glass formation is due to a reaction between BSAS and SiO_2 (grown on the Si bond coat by oxidation), forming a low melting (~1300 °C) eutectic.[10] The high velocity gas in turbine engines can blow away the low melting glass exposed on the EBC surface, causing rapid EBC recession. A continuous layer of glass along the Si/mullite + BSAS interface causes premature EBC delamination.[10] Therefore, it is desirable to avoid the BSAS component in high temperature applications (T > 1300–1350 °C) to prevent low-melting glasses.

3.2.2. Rare earth silicate EBC

Fig. 5a and b shows two typical cross-sections of Si/Yb_2SiO_5 EBC on MI SiC/SiC composite after 100 h in 90% H_2O-balance O_2 at 1300 °C (1 h cycles). The Si bond coat suffered rapid oxidation, forming a thick and sometimes porous scale (20–50 μm thick). Premature spallation of EBC occurred along the scale as the thick, porous scale constitutes a weak link. Two possible explanations for the rapid oxidation are lack of chemical bonding between Si and Yb_2SiO_5 and easy access of water vapor through cracks in Yb_2SiO_5. The fact that the Si/mullite EBC provides far superior oxidation resistance and longer life, although mullite develops similar cracks,[10] indicates that inadequate chemical bonding

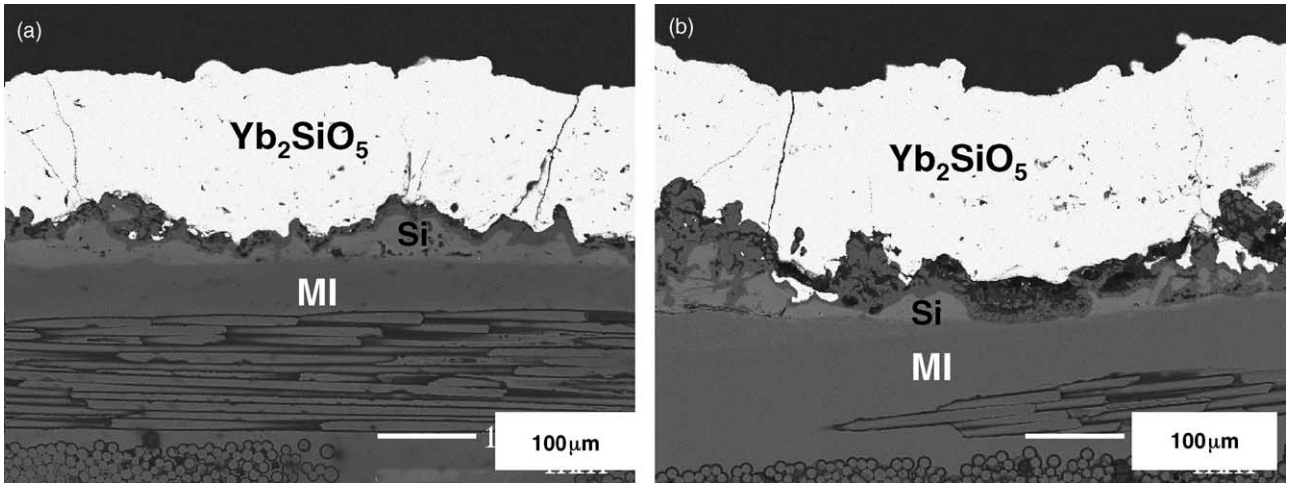

Fig. 5. Cross-sections of Si/Yb_2SiO_5 EBC on MI SiC/SiC composite after 100 h in 90% H_2O-balance O_2 at 1300 °C (1 h cycles).

is likely the more critical issue than cracks. The other rare earth silicates investigated in this study exhibited similar behavior. This necessitates an intermediate coat that provides bonding with the Si bond coat.

3.2.3. Mullite or mullite + BSAS family/rare earth silicate EBC

Fig. 6 shows the cross-section of mullite/Y_2SiO_5 EBC on SiC after 46 h in 90% H_2O-balance O_2 at 1400 °C (1 h cycles). There were severe reactions between mullite and Y_2SiO_5, turning the entire EBC into a layer of yttrium–aluminium–silicate bubbles. The Y_2O_3–Al_2O_3–SiO_2 phase diagram shows compositions with melting point as low as 1400 °C. These compositions are responsible for ternary silicate bubbles observed in the mullite/Y_2SiO_5 EBC. Adding BSAS in the mullite layer further promotes the silicate formation reaction. Ba and Sr are glass modifiers that promote glass formation and lower melting points and viscosity by breaking silica networks in glasses.[23]

Silicon/mullite + BSAS/Er_2SiO_5 EBC on MI SiC/SiC composite after 1000 h in 90% H_2O-balance O_2 at 1300 °C (1 h cycles) maintained excellent adherence and chemical compatibility, as good as the silicon/mullite + BSAS/BSAS EBC in similar exposures. Fig. 7 shows the cross-section of silicon/mullite + BSAS/Er_2SiO_5 EBC on SiC after 100 h in 90% H_2O-balance O_2 at 1400 °C (1 h cycles). Extensive erbium–aluminium–silicate glass formation is observed within the EBC as well as on the EBC surface. The low viscosity erbium–aluminium–silicate glass is responsible for interfacial pores. At 1420 °C mullite/Er_2SiO_5 EBC turned into a layer of erbium–aluminium–silicate bubbles, similar to mullite/Y_2SiO_5 EBC shown in Fig. 6. Consequently, Y_2SiO_5 or Er_2SiO_5 with mullite or mullite + BSAS family intermediate coat is not suitable for temperatures around 1400 °C or higher.

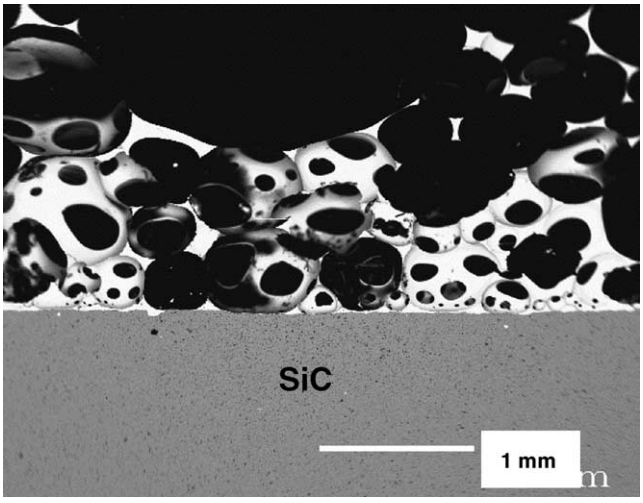

Fig. 6. Cross-section of mullite/Y_2SiO_5 EBC on SiC after 46 h in 90% H_2O-balance O_2 at 1400 °C (1 h cycles).

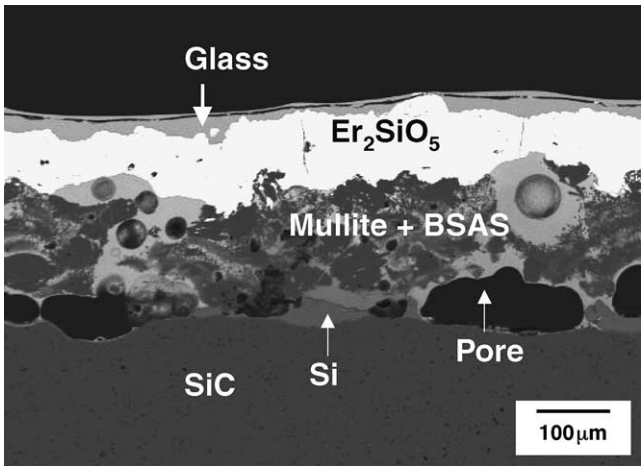

Fig. 7. Cross-section of silicon/mullite + BSAS/Er_2SiO_5 EBC on SiC after 100 h in 90% H_2O-balance O_2 at 1400 °C (1 h cycles).

Fig. 8a shows the cross-section of silicon/mullite + SAS/$Sc_2Si_2O_7$ + Sc_2O_3 EBC on MI SiC/SiC composite after 300 h in 90% H_2O-balance O_2 at 1380 °C (1 h cycles). The EBC maintained excellent adherence and chemical compatibility. The $Sc_2Si_2O_7$ + Sc_2O_3 top coat develops through-thickness cracks which typically stop in the intermediate coat or at the intermediate coat/Si bond coat interface. The slightly higher CTE of $Sc_2Si_2O_7$ + Sc_2O_3 and mullite compared to the SiC/SiC substrate (see Table 1) is mainly responsible for the through-thickness cracks. Assuming that stresses are relaxed at the high temperature during the thermal cycling, tensile stresses develop in the ceramic layers during cooling, causing the cracking. Si has lower thermal expansion than SiC (see Table 1), implying a compressive stress in the Si bond during cooling. This explains why the through-thickness cracks do not propagate into the Si bond coat. The development of compressive stress in the Si bond coat and tensile stress in the mullite intermediate coat was verified experimentally in ref.[11]

Fig. 8b and c shows high magnification views of the intermediate coat/Si bond coat interface. The thin silica scale (~2 μm) indicates excellent oxidation protection provided by the EBC (Fig. 8b). Glass formation is observed at the bottom of a crack that has penetrated to the Si bond coat/intermediate coat interface (Fig. 8c). Enhanced oxidation occurred in the area where cracks reached the Si bond coat, leading to glass formation due to the SAS-silica reaction similar to the BSAS-silica reaction described earlier. Fig. 8d is a high magnification view of the $Sc_2Si_2O_7$ + Sc_2O_3 layer. Two phases are clearly noticed: bright Sc_2O_3 precipitates and dark $Sc_2Si_2O_7$ matrix which also forms a thin surface layer (~5 μm). It is believed that the $Sc_2Si_2O_7$ surface layer is due to lower surface energy of $Sc_2Si_2O_7$ compared to Sc_2O_3. In two phase mixtures, the phase with lower surface energy moves to surfaces to minimize the surface energy.[23]

The silicon/mullite/$Sc_2Si_2O_7$ + Sc_2O_3 EBC exhibits similar behavior, except for the absence of glass formation at

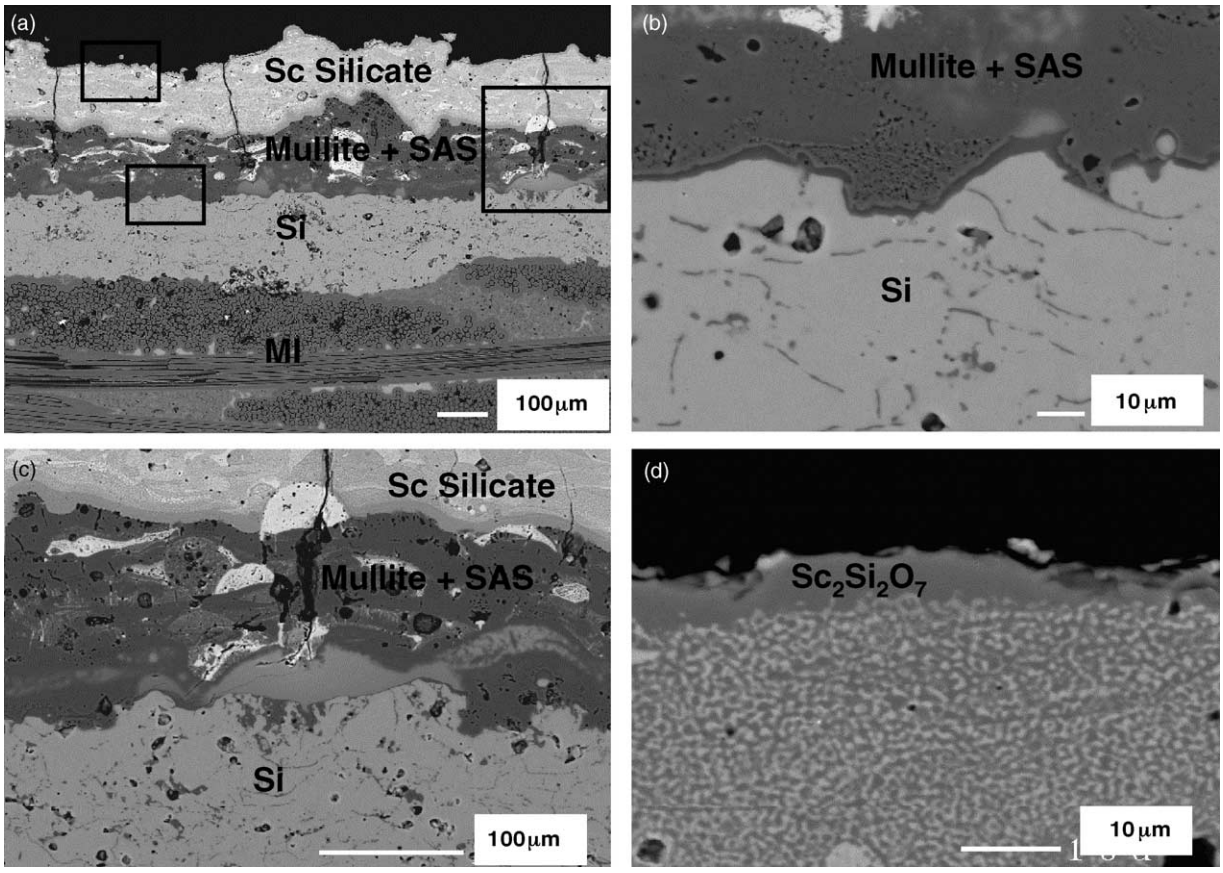

Fig. 8. Cross-section of silicon/mullite + SAS/$Sc_2Si_2O_7$ + Sc_2O_3 EBC on MI SiC/SiC composite after 300 h in 90% H_2O-balance O_2 at 1380 °C (1 h cycles).

crack tips. A mullite intermediate coat is preferable for higher temperature applications due to the absence of BSAS family-silica reaction. However, EBCs with a mullite + BSAS family intermediate coat exhibit longer durability (as long as the temperature is low enough to avoid glass formation) due to enhanced crack resistance.[10,11] The volatility of $Sc_2Si_2O_7$ phase (see Fig. 3) is expected to cause selective loss of silica from the $Sc_2Si_2O_7$ phase at high velocity combustion environments, leading to a porous Sc_2SiO_5 surface layer. Selective loss of silica from rare earth disilicates in high velocity combustion environments have been reported.[16,18,19] Porous surface layers are not likely to have sufficient mechan-

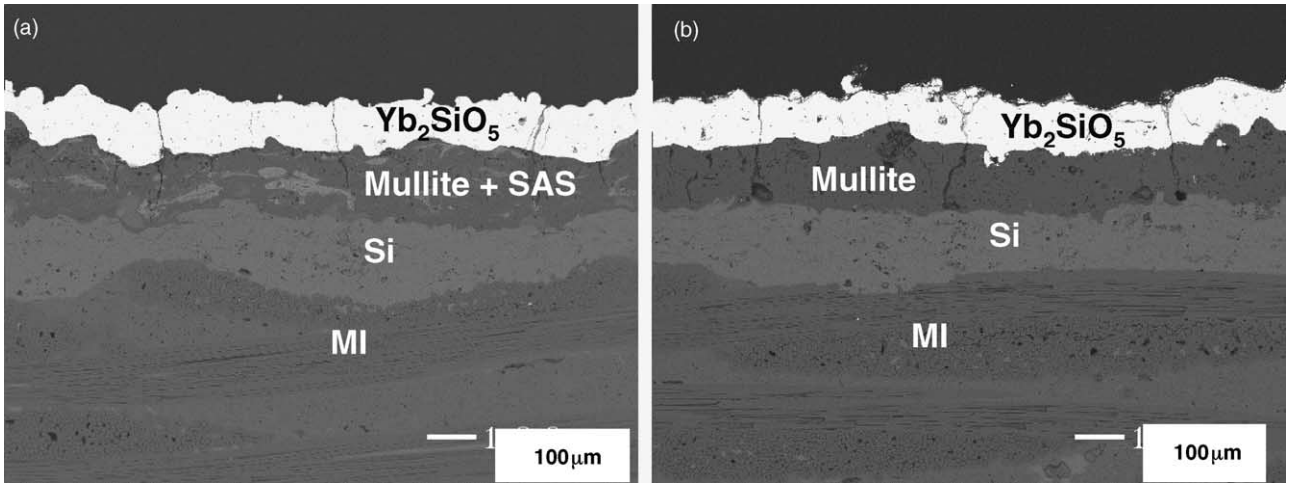

Fig. 9. Cross-sections of silicon/mullite + SAS/Yb_2SiO_5 (a) and silicon/mullite/Yb_2SiO_5 (b) EBC on MI SiC/SiC composites after 300 h in 90% H_2O-balance O_2 at 1380 °C (1 h cycles).

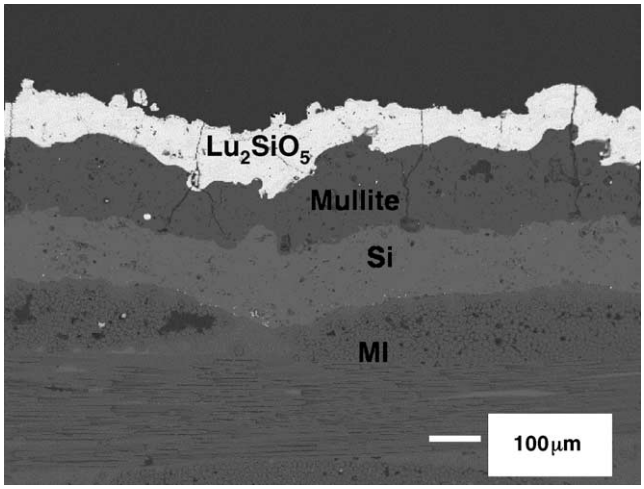

Fig. 10. Cross-section of silicon/mullite/Lu_2SiO_5 EBC on MI SiC/SiC composite after 300 h in 90% H_2O-balance O_2 at 1380 °C (1 h cycles).

ical strength and thus readily spall. Mullite exposed to high velocity combustion environments suffered a selective loss of silica, leaving a porous, easily spalling alumina surface layer.[8]

Fig. 9a and b are cross-sections of silicon/mullite + SAS/Yb_2SiO_5 and silicon/mullite/Yb_2SiO_5 EBC, respectively, on MI SiC/SiC composites after 300 h in 90% H_2O-balance O_2 at 1380 °C (1 h cycles). They exhibited excellent adherence and chemical compatibility. The through-thickness cracks tend to be narrower than in the $Sc_2Si_2O_7 + Sc_2O_3$ top coat, presumably due to the lower thermal expansion of Yb_2SiO_5 (see Table 1). Yb_2SiO_5 is expected to be less volatile than $Sc_2Si_2O_7 + Sc_2O_3$ in high velocity combustion environments as discussed earlier in the volatility section. Fig. 10 is a cross-section of silicon/mullite/Lu_2SiO_5 EBC on MI SiC/SiC composite after 300 h in 90% H_2O-balance O_2 at 1380 °C (1 h cycles). Its performance is similar to that of the silicon/mullite/Yb_2SiO_5 EBC.

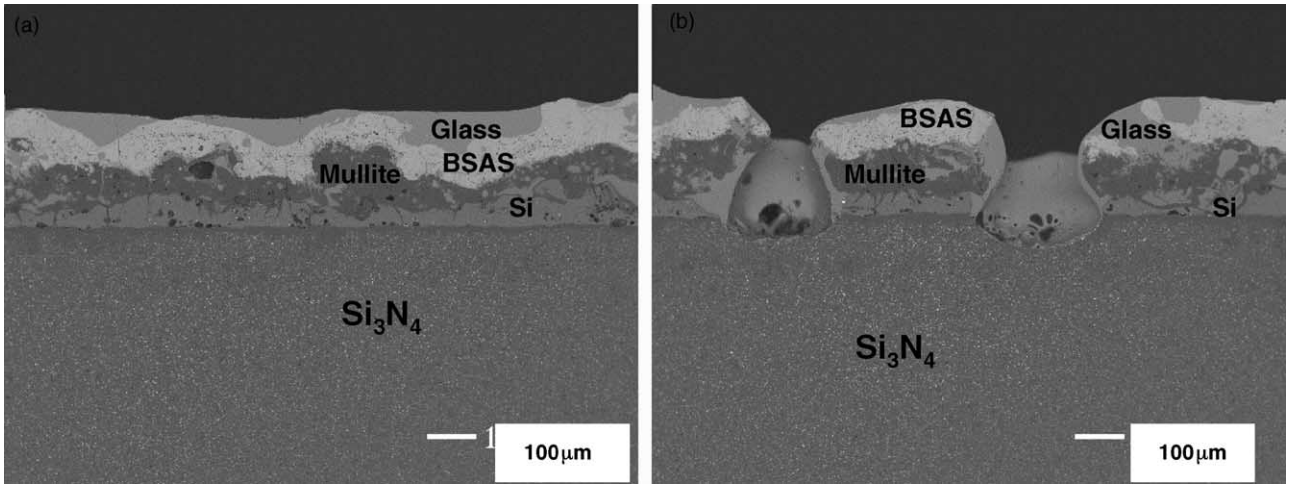

Fig. 11. Cross-sections of Si/mullite/BSAS EBC on AS800™ Si_3N_4 after 400 h in 90% H_2O-balance O_2 at 1380 °C (1 h cycles).

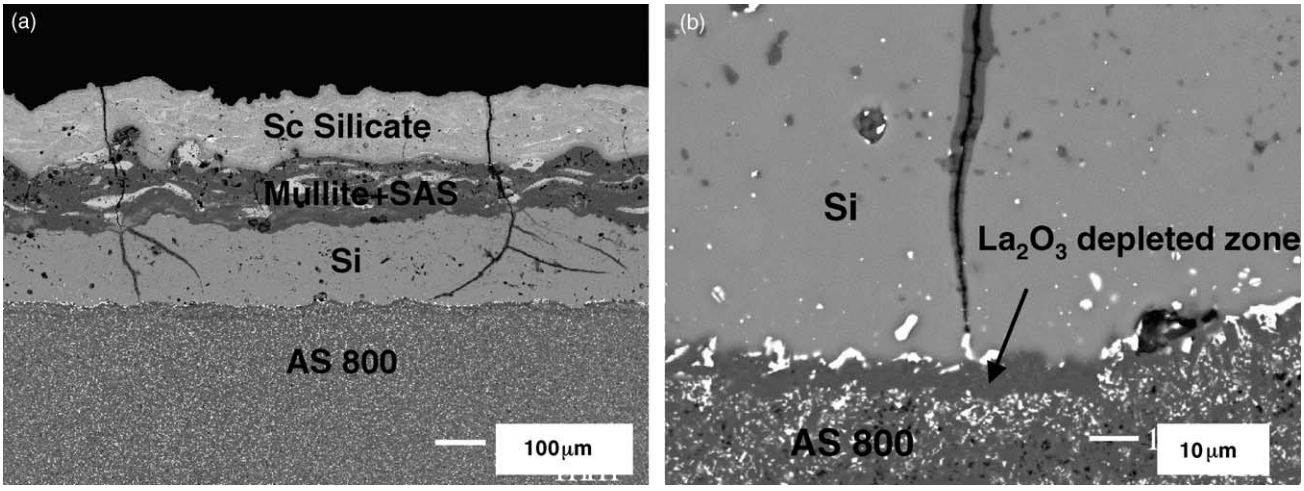

Fig. 12. Cross-sections of silicon/mullite + SAS/$Sc_2Si_2O_7 + Sc_2O_3$ EBC on AS800™ Si_3N_4 after 200 h in 90% H_2O-balance O_2 at 1380 °C (1 h cycles).

3.3. Chemical stability/environmental durability—Si_3N_4 substrate

3.3.1. Mullite or mullite + BSAS family/BSAS

Fig. 11a and b shows cross-sections of Si/mullite/BSAS EBC on AS800^{TM} Si_3N_4 after 400 h in 90% H_2O-balance O_2 at 1380 °C (1 h cycles). There was extensive formation of Ba–Sr–Al silicate glass that covered the entire EBC. The glass attacked the Si_3N_4 substrate in some areas, creating pits on the Si_3N_4 surface (Fig. 11b). This is in contrast to the same coating on SiC or SiC/SiC composites in which no significant glass formation occurs after similar exposures.[10] The glass formation was far more severe with a mullite + BSAS intermediate coat. La_2O_3 and SrO additives in the AS800^{TM} Si_3N_4 reach the EBC and promote the glass formation reaction even in the absence of BSAS in the intermediate layer.

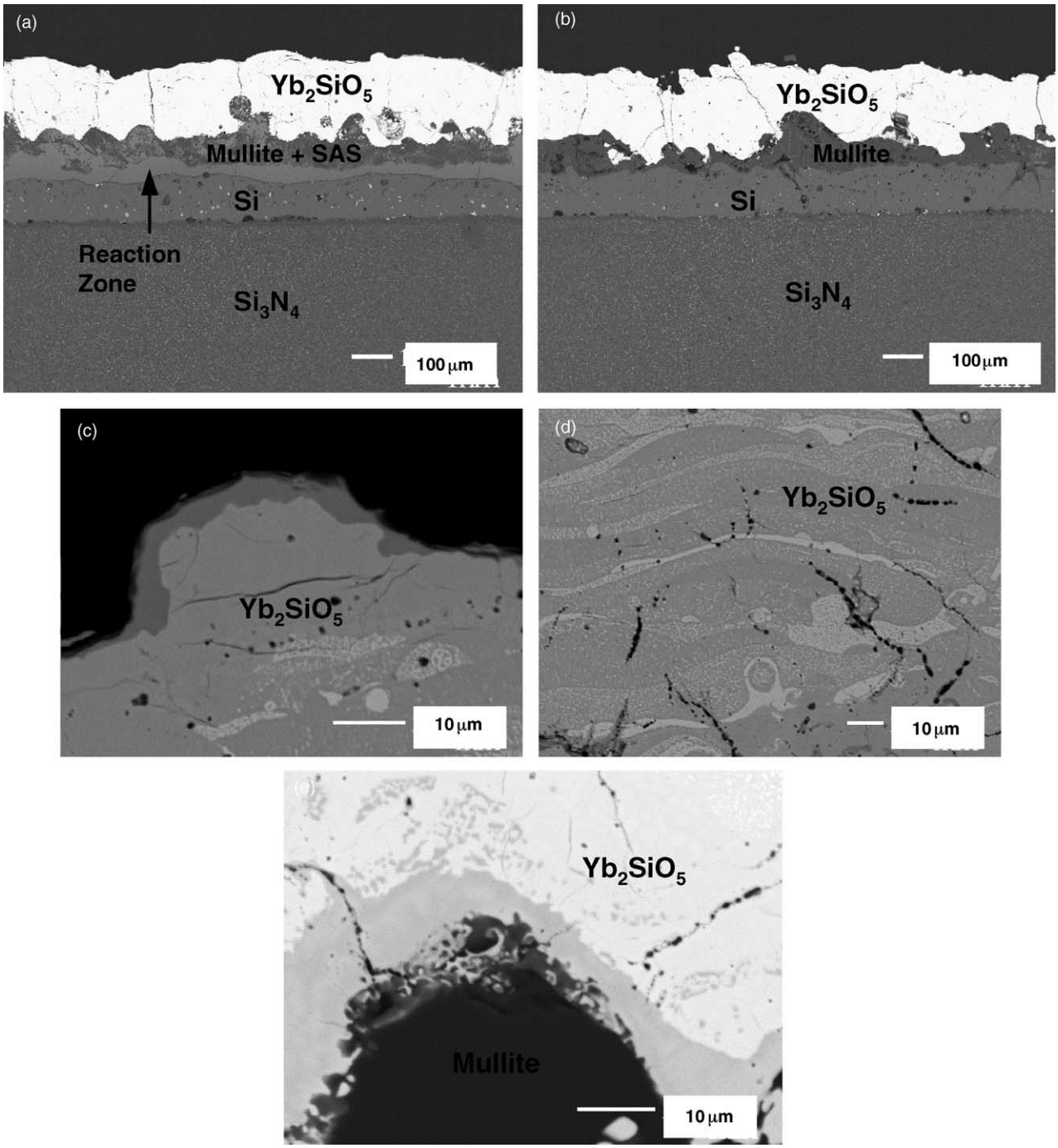

Fig. 13. Cross-sections of silicon/mullite + SAS/Yb_2SiO_5 (a) and silicon/mullite/Yb_2SiO_5 (b) EBC on AS800^{TM} Si_3N_4 after 400 h in 90% H_2O-balance O_2 at 1380 °C (1 h cycles).

EDS analysis of the glass layer confirmed the presence of La, while Sr could not be confirmed since its peak overlaps with the Si peak.

3.3.2. Mullite or mullite + BSAS family/rare earth silicates EBC

Fig. 12a and b shows cross-sections of silicon/mullite + SAS/$Sc_2Si_2O_7$ + Sc_2O_3 EBC on AS800^{TM} Si_3N_4 after 200 h in 90% H_2O-balance O_2 at 1380 °C (1 h cycles). The EBC exhibited excellent adherence and chemical compatibility. In contrast to the same EBC on MI SiC/SiC composites in which cracks stop within the intermediate coat or at the intermediate coat/Si bond coat interface, cracks typically penetrate through the Si bond coat all the way to the Si/Si_3N_4 interface. Some cracks branch laterally within the Si bond coat. The disparity in the cracking behavior can be explained by the difference in thermal expansion between MI SiC/SiC and Si_3N_4. As discussed earlier Si has lower thermal expansion than MI SiC/SiC composites. Thus, the Si bond coat on MI is in compression, preventing the crack penetration. In contrast, Si has higher thermal expansion than Si_3N_4 (see Table 1), implying a tensile stress in the Si bond coat. Consequently, cracks can readily propagate through the Si bond coat. Oxidation occurs on crack surfaces (Fig. 12b), accelerating the degradation of the Si bond coat. The cracks branching laterally can be interconnected to form long horizontal cracks, leading to premature EBC delamination. Therefore, the cracking behavior in the Si bond coat on Si_3N_4 is deleterious to the durability of EBC, especially under frequent thermal cycles. There weren't noticeable chemical reactions at the intermediate coat/bond coat interface despite the presence of SAS in the intermediate coat. This is in contrast to the massive glass formation in the mullite or mullite + BSAS family/BSAS-coated AS800^{TM} Si_3N_4. The lack of glass formation with the $Sc_2Si_2O_7$ + Sc_2O_3 top coat indicates a critical role by the BSAS top coat in the glass formation reaction.

Fig. 13a and b shows cross-sections of silicon/mullite + SAS/Yb_2SiO_5 and silicon/mullite/Yb_2SiO_5 EBC, respectively, on AS800^{TM} Si_3N_4 after 400 h in 90% H_2O-balance O_2 at 1380 °C (1 h cycles). There are two features distinctively different from the behavior of EBC having a $Sc_2Si_2O_7$ + Sc_2O_3 top coat (Fig. 12a): (i) through-thickness cracks are narrower with less penetration to the Si bond coat; (ii) substantial chemical reaction at the mullite + SAS intermediate coat/Si bond coat interface, forming a continuous interfacial glass layer. The fact that there was no glass formation in the Si/mullite/Yb_2SiO_5 or Si/mullite + SAS/$Sc_2Si_2O_7$ + Sc_2O_3 EBCs indicates that the presence of both Yb_2SiO_5 and SAS is needed for the enhanced glass formation shown in Fig. 13b. This may indicate that Yb_2SiO_5 is more reactive with BSAS family than $Sc_2Si_2O_7$ + Sc_2O_3. It is also interesting to note that the silicon/mullite + SAS/Yb_2SiO_5 EBC on SiC/SiC composites did not form glasses (Fig. 9a). This supports the earlier suggestion that the additives in AS800^{TM} Si_3N_4 promote glass formation. The narrower crack width is attributed to two factors: the lower thermal expansion of Yb_2SiO_5 compared to $Sc_2Si_2O_7$ + Sc_2O_3 and thinner intermediate coat (compare Figs. 12a and 13a). Both the lower thermal expansion of Yb_2SiO_5 and the thinner intermediate coat contribute to reducing the EBC strain (tensile).

Fig. 13c–e shows higher magnification views of the top coat surface, the top coat mid section, and the top coat/mullite interface after the 400-h exposure. Three phases are clearly noticed in the top coat: a dark surface layer, small bright precipitates, and the matrix with an intermediate contrast. Both Yb_2SiO_5 and $Yb_2Si_2O_7$ were major phases according to X-ray diffraction. Judging from XRD and EDS analysis, it is believed that the dark surface layer is $Yb_2Si_2O_7$, bright precipitates are Yb_2O_3 and the matrix is Yb_2SiO_5. Therefore, Yb_2SiO_5 is the major phase with a small amount of Yb_2O_3 precipitates and a thin layer of $Yb_2Si_2O_7$ surface layer. As discussed with respect to scandium silicate, the presence of

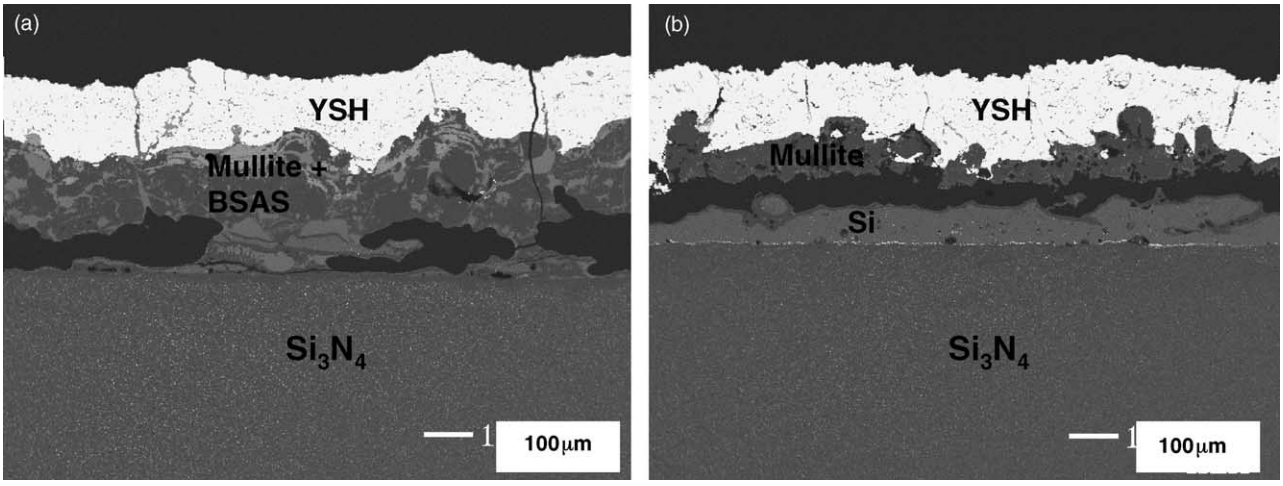

Fig. 14. Cross-sections of silicon/mullite + BSAS/yttria-stabilized HfO_2 (a) and silicon/mullite/yttria-stabilized HfO_2 (b) EBC on AS800^{TM} Si_3N_4 after 200 and 300 h, respectively, in 90% H_2O-balance O_2 at 1380 °C (1 h cycles).

$Yb_2Si_2O_7$ on the surface is presumably due to its low surface energy. There was a limited diffusion reaction (5–10 μm thick) at the Yb_2SiO_5/mullite interface, which is not likely to affect the EBC durability (Fig. 13e).

3.3.3. Mullite or mullite + BSAS family/yttria-stabilized hafnia EBC

Fig. 14a and b shows cross-sections of silicon/mullite + BSAS/yttria-stabilized HfO_2 and silicon/mullite/yttria-stabilized HfO_2 EBC on AS800^{TM} Si_3N_4 after 200 and 300 h, respectively, in 90% H_2O-balance O_2 at 1380 °C (1 h cycles). Both EBCs were severely delaminated and spalled either along the intermediate coat/Si bond coat interface or at the Si/Si_3N_4 interface. Significant glass formation is observed within the mullite + BSAS intermediate coat. The severe delamination is ascribed to the high CTE of yttria-stabilized hafnia ($\sim 10 \times 10^{-6}$ °C),[24] leading to a high tensile strain. Similar behavior was observed with silicon/mullite or mullite + BSAS/yttria-stabilized ZrO_2 EBC on AS800^{TM} Si_3N_4. It has been shown that Si/mullite + BSAS/yttria-stabilized zirconia EBC on SiC generates much higher tensile stress than Si/mullite + BSAS/BSAS EBC due to the high CTE mismatch and YSZ sintering.[11] The high strain resulted in premature EBC failure under thermal cycling.

4. Conclusions

Our volatility data in conjunction with thermodynamic calculations[22] in the literature indicate that rare earth monosilicates are less volatile than BSAS and rare earth disilicates in combustion environments. Some rare earth silicates, such as ytterbium, lutetium, and scandium silicates, are chemically more stable than BSAS. One potential disadvantage of rare earth silicate coatings compared to BSAS coating is their susceptibility to through-thickness cracking. Through-thickness cracks, however, may not be a concern for EBCs on SiC/SiC composites in which the cracks typically stop within the intermediate coat or at the intermediate/bond coat interface. On Si_3N_4 substrates cracks tend to propagate all the way to the Si bond coat/substrate interface. This may affect the long-term durability under frequent thermal cycling. The cracking was significantly reduced with a lower CTE rare earth silicate top coat, such as Yb_2SiO_5, and a thinner mullite-based intermediate coat. Thermal cycling tests in simulated combustion environments have demonstrated the potential of rare earth monosilicate EBC (Yb_2SiO_5, Sc_2SiO_5, Lu_2SiO_5) for advanced gas turbine engines requiring higher temperature capability and durability than current EBCs.

References

1. Opila, E. J. and Hann, R., Paralinear oxidation of CVD SiC in water vapor. *J. Am. Ceram. Soc.*, 1997, **80**(1), 197–205.
2. Smialek, J. L., Robinson, R. C., Opila, E. J., Fox, D. S. and Jacobson, N. S., SiC and Si_3N_4 scale volatility under combustor conditions. *Adv. Compos. Mater.*, 1999, **8**(1), 33–45.
3. Lee, K. N., Fritze, H. and Ogura, Y., Coatings for engineering ceramics; in progress. In *Ceramic Gas Turbine Development, Vol 2*, ed. M. van Roode, M. Ferber and D. W. Richerson. ASME Press, New York, NY, 2003.
4. Richerson, D. W. and Schienle, J. L., High temperature coating study to reduce contact stress damage to ceramics. In *Proceedings of the Twenty-Second Automotive Technology Development Contractors' Coordination Meeting*, 1985.
5. Price, J. R., van Roode, M. and Stala, C., Ceramic oxide-coated silicon carbide for high temperature corrosive environments. *Key Eng. Mater.*, 1992, **72–74**, 71–84.
6. Federer, J. I., Alumina base coatings for protection of SiC ceramics. *J. Mater. Eng.*, 1990, **12**, 141–149.
7. Lee, K. N., Miller, R. A. and Jacobson, N. S., New generation of plasma-sprayed mullite coatings on silicon-carbide. *J. Am. Ceram. Soc.*, 1995, **78**(3), 705–710.
8. Lee, K. N., Key durability issues with mullite-based environmental barrier coatings for Si-based ceramics. *Trans. ASME*, 2000, **122**, 632–636.
9. Lee, K. N., Current status of environmental barrier coatings for Si-based ceramics. *Surf. Coat. Technol.*, 2000, **1–7**, 133–134.
10. Lee, K. N., Fox, D. S., Eldridge, J. I., Zhu, D., Robinson, R. C., Bansal, N. P. *et al.*, Upper temperature limit of environmental barrier coatings based on mullite and BSAS. *J. Am. Ceram. Soc.*, 2003, **86**(8), 1299–1306.
11. Lee, K. N., Eldridge, J. I. and Robinson, R. C., Stress evolution and its effects on the durability of environmental barrier coatings for SiC ceramics, *J. Am. Ceram. Soc.*, submitted for publication.
12. Eaton, H. E., Linsey, G. D., Sun, E. Y., More, K. L., Kimmel, J. B., Price, J. R. *et al.*, EBC protection of SiC/SiC composites in the gas turbine combustion environment—continuing evaluation and refurbishment considerations. ASME paper 2001-GT-0513 ASME TURBOEXPO 2001. June 4–7, 2001. New Orleans, Louisiana.
13. More, K. L., Tortorelli, P. F., Walker, L. R., Kimmel, J. B., Miriyala, N., Price, J. R. *et al.*, Evaluating environmental barrier coatings on ceramic matrix composites after engine and laboratory exposures. ASME paper 2002-GT-30630. In *Proceedings of ASME Turbo Expo 2002*, June 3–6, 2002. Amsterdam, The Netherlands.
14. Maqsood, A., Wanklyn, B. M. and Garton, G., *J. Cryst. Growth*, 1979, **46**, 672.
15. Liddell, K. and Thompson, D. P., X-ray diffraction data of yttrium silicates. *Br. Ceram. Trans. J.*, 1986, **85**, 17–22.
16. Ohji, T., Environmental barrier coating on silicon nitride; challenges and critical issues. In *Proceedings of the 28th Int. Conf. & Exp. On Adv. Ceram. & Composites*, 2004.
17. Felshe, J., *Structure & Bonding*, 1973, **13**, 100.
18. Klemm, H., Fritsch, M. and Schenk, B., Corrosion of ceramic materials in hot gas environments. In *Proceedings of the 28th Int. Conf. & Exp. On Adv. Ceram. & Composites*, 2004.
19. Ueno, S., Jayaseelan, D. D., Kondo, N., Ohji, T. and Kanzaki, S., High temperature water vapor corrosion resistance of silicon nitride with Lu–Si–O EBC layer. In *Proceedings of the 28th Int. Conf. & Exp. On Adv. Ceram. & Composites*, 2004.
20. Brewer, D., HSR/EPM combustor materials development program. *Mater. Sci. Eng., A*, 1999, **261**, 284–291.
21. Opila, E. J. and Meyers, D. L., *Alumina Volatility in Water Vapor at Elevated Temperatures: Application to Combustion Environments High Temperature Corrosion and Materials Chemistry*. The Electrochemical Society, Pennington, NJ, 2003, pp. 535–544.
22. Meschter, P., GE Global Research Center, private communication.
23. Kingery, W. D., Bowen, H. K. and Uhlmann, D. R., *Introduction to Ceramics* (*2nd ed.*). John Wiley & Sons, New York, 1975.
24. Touloukian, Y. S., Kirby, R. K., Taylor, R. E. and Lee, T. Y. R., *Thermophysical Properties of Matter, Vol 13*. IFI/Plenum, New York, 1977.